Supplementary Information

Self-trapped exciton emission and piezochromism in conventional 3D lead bromide perovskite nanocrystals under high pressure

Yue Shi, Wenya Zhao, Zhiwei Ma, Guanjun Xiao* and Bo Zou

State Key Laboratory of Superhard Materials, College of Physics, Jilin University, Changchun 130012, China.

*Corresponding Author E-mail: xguanjun@jlu.edu.cn

Table of Contents

EXPERIMENTAL DETAILS

Materials.

Cesium carbonate (Cs_2CO_3, 99% metals basis, Sigma-Aldrich), lead (II) bromide ($PbBr_2$, puratronic 99.999% metals basis, Alfa Aesar), manganese (II) bromide ($MnBr_2$, anhydrous, 99%, Alfa Aesar), hydrobromic acid (HBr, ACS grade 47-49%, Alfa Aesar), oleylamine (Olam, technical grade 70%, Aldrich), oleic acid (OA, technical grade 90%, Sigma-Aldrich), 1-octadecene (ODE, technical grade 90%, Sigma-Aldrich).

Preparation of Cs-Oleate.

0.125 g of Cs_2CO_3 was loaded in a 50 mL three-neck flask together with 4.5 mL of ODE and 0.45 mL of OA. The mixture was stirred for 1 h at 150 ℃, followed by cooled down to 110 ℃ under N_2 until the further use.

Typical synthesis of $CsPb_xMn_{1-x}Br_3$ NCs.

$CsPb_xMn_{1-x}Br_3$ NCs was synthesized via hot-injection method similar to a modified synthetic approach. [1] Typically, 0.058 g $PbBr_2$, 0.1696 g $MnBr_2$, 5 mL of ODE, along with 0.7 mL of Olam, 0.7 mL of OA and 200 μL were loaded in a 50 mL three-neck flash, and dried under N_2 for 1 h at 120 ℃. Until $PbBr_2$ and $MnBr_2$ were completely dissolved, the solution was heated under N_2 to 200 ℃. Then, additional 0.7 mL OA and 0.7 mL Olam were injected until the temperature was stable. Then, 0.4 ml of hot 110 ℃ Cs-oleate precursor was rapidly injected into the reaction mixture. About 10 s after injection, the reaction mixture was quenched by the ice-water bath.

Purification.

The $CsPb_xMn_{1-x}Br_3$ NCs was centrifuged twice by adding hexane and toluene centrifuging for 10 mins at 3500 rpm.

High pressure generation.

High-pressure were generated by a symmetric diamond anvil cell (DAC) with a culet size of 400 μm. Then we drilled a 150 μm-diameter hole in the center of T301 stainless steel gasket as the sample chamber, which was preindented to 45 μm. The sample and a small ruby ball were loaded into the gasket cavity. The standard ruby fluorescent technique was carried out to determine the actual pressure. Silicon oil (Dow

Corning Corporation, 10 cSt) was used as the pressure transmitting medium to provide the hydrostaticity.

PL and absorption spectra.

The in situ high-pressure PL and absorption spectra were collected with the help of an optical fiber spectrometer (Ocean Optics, QE65000). The pressure-dependent PL spectra were measured by a semiconductor laser with an excitation wavelength of 355 nm. We took the PL micrographs of the samples upon compression with a camera (Canon Eos 5D mark II) installed on a microscope (Ecilipse TI-U, Nikon). A deuterium-halogen light source was used for the absorption measurements during the whole compression.

ADXRD patterns.

In situ high-pressure angle-dispersive X-ray diffraction (ADXRD) patterns were measured at beamline 15U1, Shanghai Synchrotron Radiation Facility (SSRF). Portions of this work were performed at 4W2HP-Station, Beijing Synchrotron Radiation Facility (BSRF). The monochromatic wavelength of the synchrotron radiation was 0.6199 Å and we used CeO_2 as the standard sample for the calibration. The pattern of intensity versus diffraction angle 2θ was plotted based on the FIT2D program, which integrated and analyzed the 2D images collected. All the high-pressure experiments were conducted at room temperature.

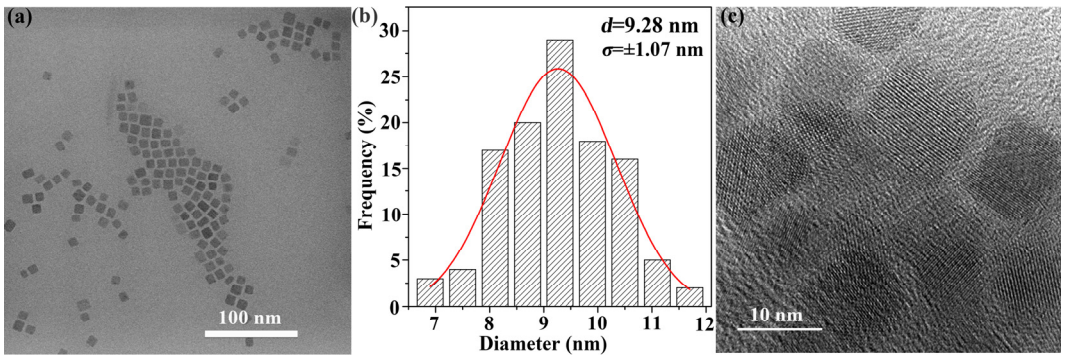

Figure S1. (a) TEM image and (b) the corresponding size distribution of as-prepared Mn-doped $CsPbBr_3$ NCs with Gauss fitting. (c) High-resolution TEM (HRTEM) image of Mn-doped $CsPbBr_3$ NCs before compression.

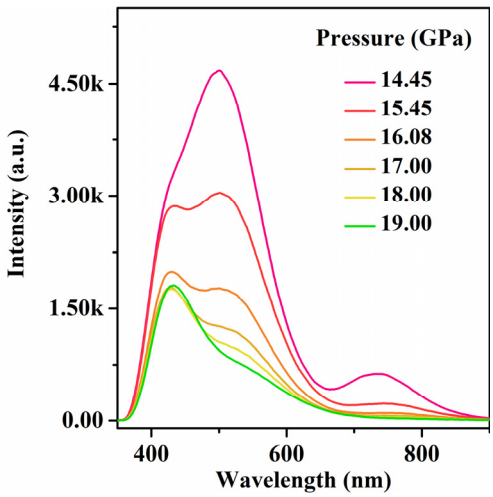

Figure S2. PL spectra of Mn-doped $CsPbBr_3$ NCs under high pressure.

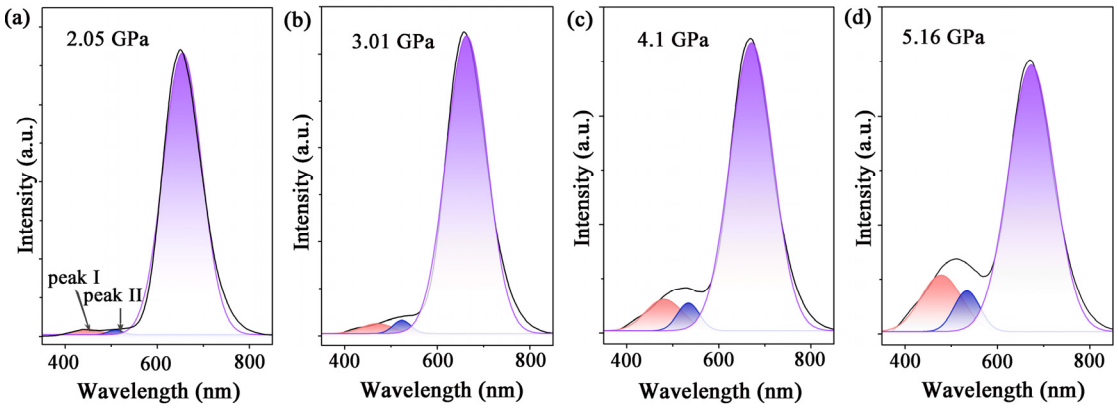

Figure S3. PL spectra fitting of Mn-doped $CsPbBr_3$ NCs by using Gaussian functions at 2.05 GPa (a), 3.01 GPa (b), 4.10 GPa (c) and 5.16 GPa (d). Peak I and II are represented by pink and blue, which are classified as self-trapped emission peaks. Peak III is represented by purple line which is Mn-related emission.

Table S1. Information about the fitted three peaks with pressure of Mn-doped $CsPbBr_3$ NCs.

Pressure (GPa)	Peak I (nm)	Intensity	FWHM (nm)	Peak II (nm)	Intensity	FWHM (nm)	Peak III (nm)	Intensity	FWHM (nm)
2.05	448.57	68.70	64.58	508.74	62.44	37.80	654.36	3646.48	97.62
3.01	469.76	105.03	81.08	523.26	140.02	45.27	663.04	3468.62	103.03
4.10	480.68	287.21	93.13	533.52	252.55	55.89	670.69	2653.80	109.23
5.16	477.80	518.42	103.08	533.62	372.55	65.32	672.93	2448.40	115.34

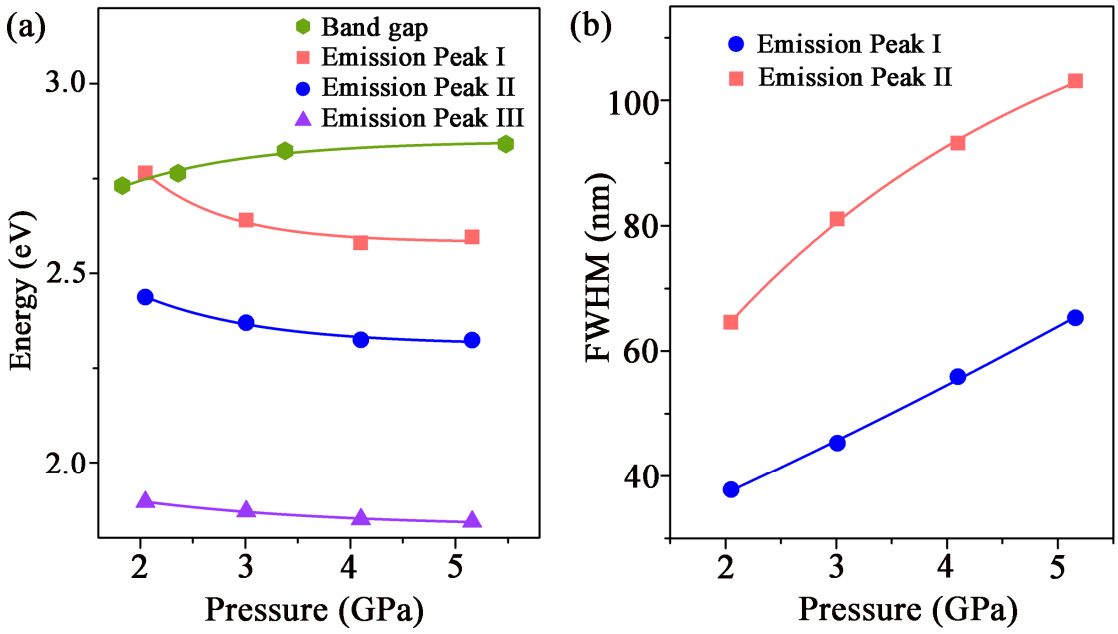

Figure S4. (a) Peak position changes of the fitted three peaks and band gap values with pressure. (b) Changes of FWHM of selected Peak I and II with increase in pressure.

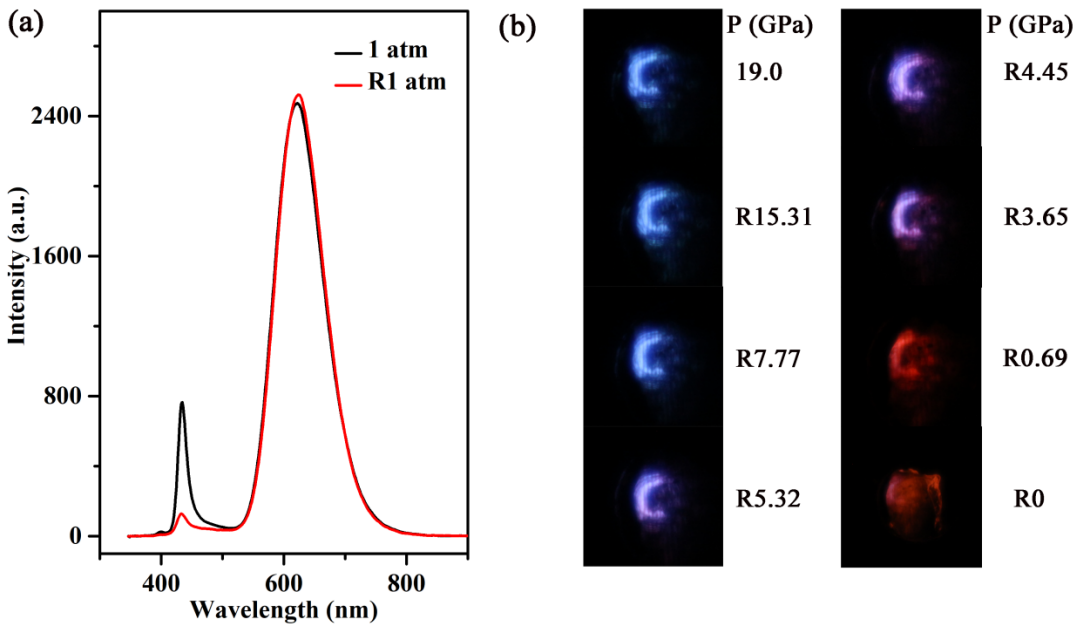

Figure S5. (a) Comparison of PL emission between 1 atm and decompression of Mn-doped $CsPbBr_3$ NCs. (b) PL micrographs with decreasing pressure.

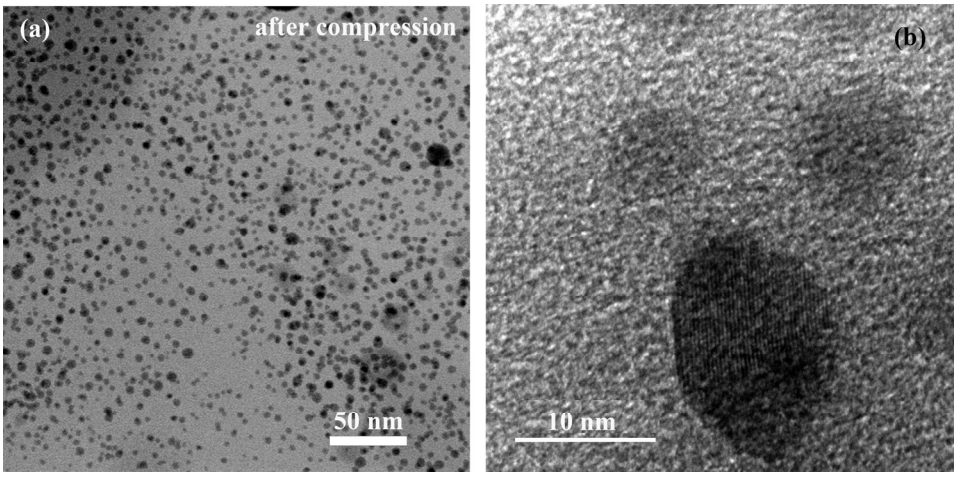

Figure S6. (a) TEM image and (b) HRTEM image of the obtained Mn-doped $CsPbBr_3$ NCs when the pressure was completely released to ambient conditions from 21.75 GPa.

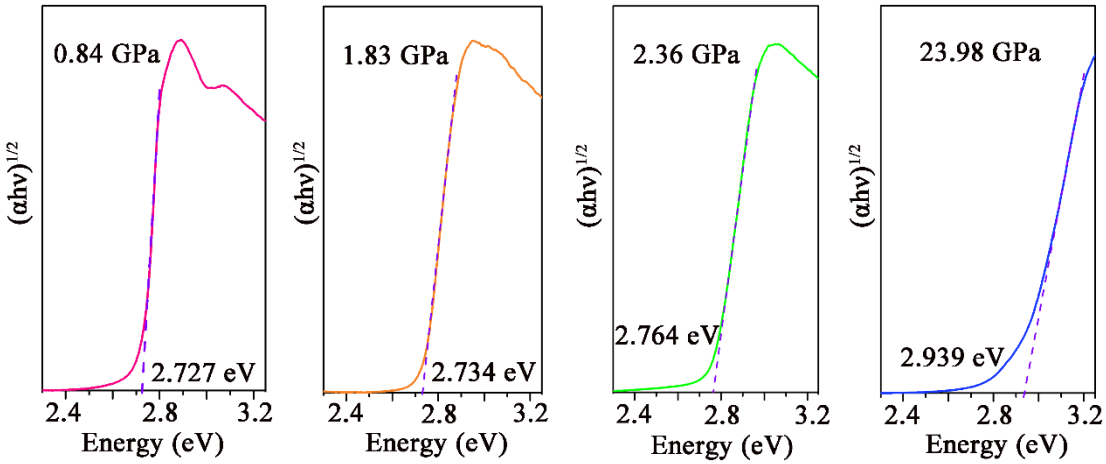

Figure S7. Band gaps of $CsPb_xMn_{1-x}Br_3$ NCs at selected pressures of 0.84, 1.83, 2.36 and 23.98 GPa estimated by the Tauc plot.

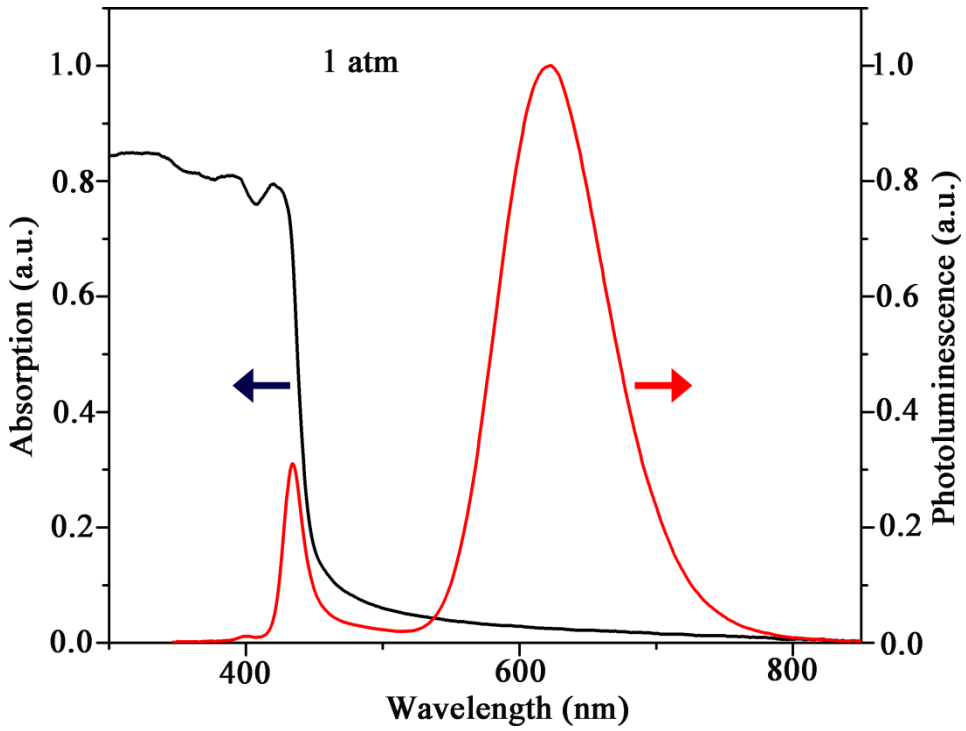

Figure S8. Absorption and PL spectra of Mn-doped $CsPbBr_3$ NCs at ambient condition.

However, to further analyze the structural evolution, the changes of lattice constants of $CsPb_xMn_{1-x}Br_3$ NCs upon compression were simply expounded (Figure 3b-e). It was found that the pressure response of the *c* axis was more sensitive to the pressure compared with the *a* and *b* axes, but the compressibility *a* and *b* axes for $CsPb_xMn_{1-x}Br_3$ NCs was similar (Figure 3d and e). Meanwhile, the compressed rate happened to be a turning point for the b axis at above 2.05 GPa. High pressure compressibilities were calculated following the equation below:

$$K_l = -(\frac{\partial l}{\partial p})_T \quad (1)$$

where l is the axial length of materials under pressure. This parameter is widely used to evaluate the pressure sensitivity and contraction ability of the structure along the specific direction. Furthermore, the experimental pressure− volume (P−V) data (Figure 3c) ranging from ambience to 19.9 GPa were fitted utilizing the following third-order Birch− Murnaghan equation of state:

$$P(V) = \frac{3B_0}{2}\left[\left(\frac{V_0}{V}\right)^{7/3} - \left(\frac{V_0}{V}\right)^{5/3}\right]\left\{1 + \frac{3}{4}(B_0' - 4)\left[\left(\frac{V_0}{V}\right)^{2/3} - 1\right]\right\} \quad (2)$$

where V_0 is the zero-pressure volume, B_0 is the bulk modulus at ambient pressure, and B_0' is a parameter for the pressure derivative. No further discontinuities were apparent in the P−V profile over the whole compression. Nevertheless, a significant change could be observed in compressibility at 2.05 GPa, which well agrees with the evolution of the absorption and PL spectra. Since the isostructural phase transitions are usually considered to originate from the electronic structural change in the matter, the as-prepared $CsPb_xMn_{1-x}Br_3$ NCs do undergo an isostructural phase transition. The physical origin points to the repulsive force impact because of the overlap between the valence electron charge clouds of the neighboring layers. With B_0' fixed at 4, the isothermal bulk modulus B_0 for phase II of $CsPb_xMn_{1-x}Br_3$ NCs was estimated as 99.48(2) GPa, which is much larger than that of phase I (14.91(9) GPa). This finding indicates the highly difficult compressibility toward phase II.

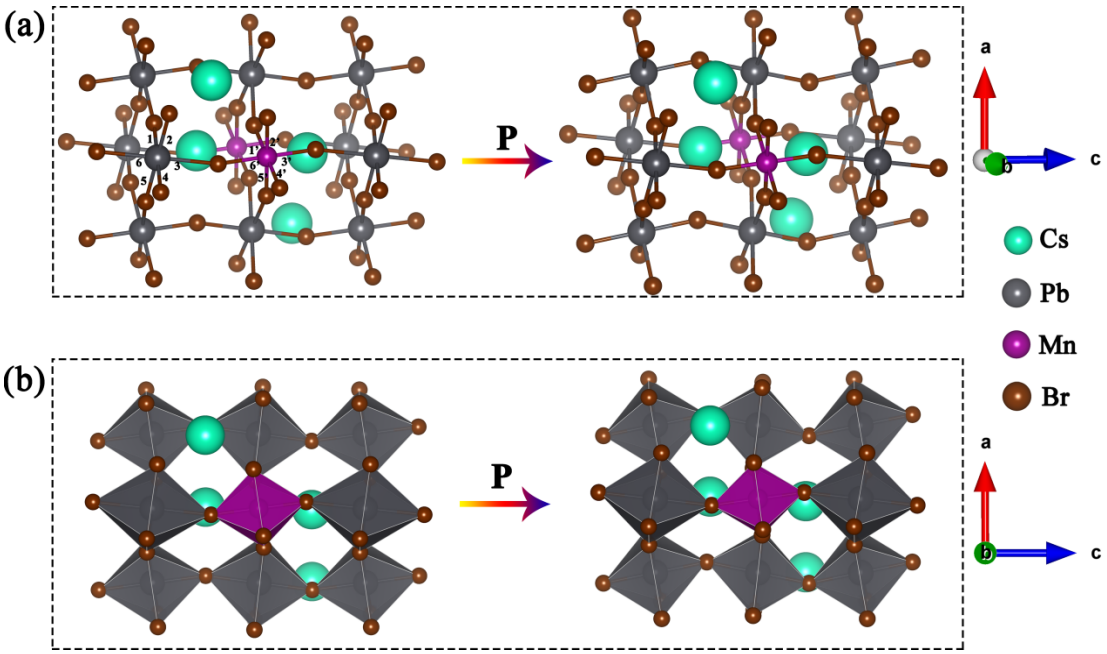

Figure S9. (a) Ball and stick model of $CsPb_xMn_{1-x}Br_3$ NCs at 1 atm and high pressure. Number 1 to 6 of the Pb-Br bond and 1' to 6' of the Mn-Br bond consistent with the Table S2. (b) Octahedral model corresponding to (a).

We compared the optimized structures of different pressure points and found that the degree of distortion of the Pb and Mn octahedron are not the same (Figure S9). The corresponding bond length of Pb-Br and Pb-Mn were summarized in the Table S2. We found that the bond length were reduced unevenly which causes uneven distortion of the crystal lattice (Figure 4).

Table S2. Bond length of $CsPb_xMn_{1-x}Br_3$ at 1 atm and 2.36 GPa. Number 1 to 6 of the bond constants with the Figure S9a

	1 atm		2.36 GPa	
	Pb-Br	Mn-Br	Pb-Br	Mn-Br
Bond 1	3.0085(8)	2.7580(0)	2.9463(6)	2.6969(0)
Bond 2	3.0042(6)	2.7598(6)	2.8997(3)	2.6010(0)
Bond 3	3.1605(1)	2.7198(4)	2.9930(7)	2.6156(5)
Bond 4	3.0080(8)	2.7573(0)	2.9792(6)	2.7935(2)
Bond 5	3.0039(8)	2.7591(0)	3.0202(5)	2.7953(3)
Bond 6	3.1601(7)	2.7797(1)	2.9915(4)	2.6005(2)

References

1. D. Parobek, Y. Dong, T. Qiao, D. H. Son, *Chem. Mater.* 2018, **30**, 2939-2944.